CZECH TECHNICAL UNIVERSITY IN PRAGUE

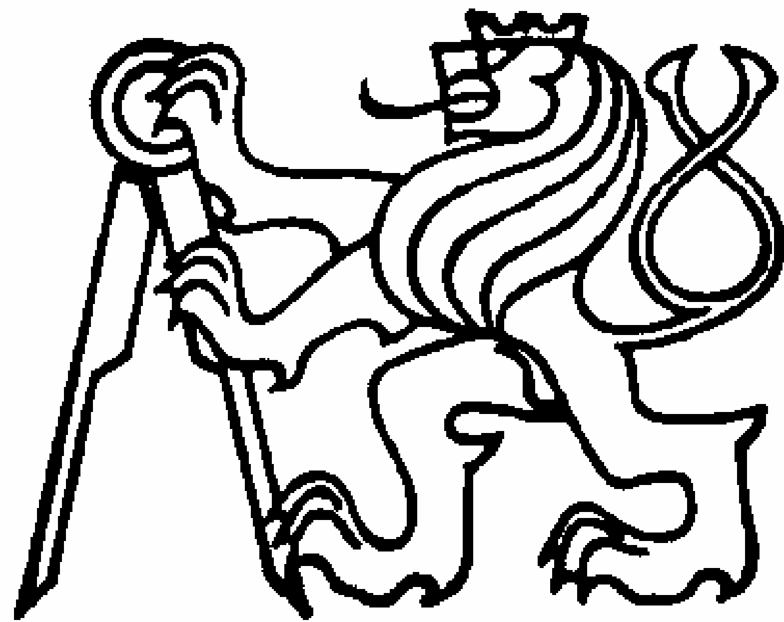

DOCTORAL THESIS STATEMENT

Czech Technical University in Prague

Faculty of Electrical Engineering

Department of Microelectronics

Ján Scheirich

THE DEPFET PARTICLE DETECTOR SYSTEMS AND THEIR CHARACTERIZATION

Ph.D. Programme: Electrical Engineering and Information Technology

Branch of study: Electronics

Doctoral thesis statement for obtaining the academic title of “Doctor”, abbreviated to “Ph.D.”

Prague, November 2012

The doctoral thesis was produced in full-time manner

Ph.D. study at the department of Microelectronics of the Faculty of Electrical Engineering of the CTU in Prague

Candidate: **Ján Scheirich**
Department of Microelectronics
Faculty of Electrical Engineering of the CTU in Prague
Technická 2, 166 27 Prague 6

Supervisor: **Prof. Ing. Miroslav Husák, PhD.**
Department of Microelectronics
Faculty of Electrical Engineering of the CTU in Prague
Technická 2, 166 27 Prague 6

Supervisor-Specialist: **RNDr. Peter Kodyš, PhD.**
Institute of Particle and Nuclear Physics
Faculty of Mathematics and Physics of the CUNI in Prague
V Holešovickách 2, 180 00 Prague 8

Opponents:

The doctoral thesis statement was distributed on:

The defence of the doctoral thesis will be held on ____ at ____ a.m./p.m. before the Board for the Defence of the Doctoral Thesis in the branch of study Electronics in the meeting room No. _____ of the Faculty of Electrical Engineering of the CTU in Prague.

Those interested may get acquainted with the doctoral thesis concerned at the Dean Office of the Faculty of Electrical Engineering of the CTU in Prague, at the Department for Science and Research, Technická 2, Prague 6.

Chairman of the Board for the Defence of the Doctoral Thesis
in the branch of study Electronics
Faculty of Electrical Engineering of the CTU in Prague

Technická 2, 166 27 Prague 6.

Summary

An upgrade of the Belle KEK B-Factory particle experiment, Belle II, is being proceeded in Japan. Collisions of asymmetric electron and positron beam are used for production of pairs of B and anti-B mesons. Belle II experiment plans to confirm the existence of new particles by studies of flavour physics reactions with high statistics. The new type of semiconductor pixel detector the DEPFET (DEPleted Field Effect Transistor) proposed by Kemmer and Lutz in 1987 is being used in the Belle II detector measuring type, track, momentum and energy of the newly-originated particles. The DEPFET sensor has a MOSFET (Metal Oxide Semiconductor Field Effect Transistor) integrated in each pixel and introduces new concept of active pixels with low noise at room temperature, non-destructive repetitive readout and thinned technologies.

The DEPFET test system called Mini-matrix system was designed for testing and characterization of small DEPFET prototypes. The system has overall noise around 20 electrons of equivalent input referred noise charge. It can drive sensors with 48 active pixels by the reconfigurable steering sequences with high time resolution. The test system integrates a computer controlled positioning of a laser beam focuser which can scan the detector surface and computer controlled power supplies, so automated tests can be performed. The system is placed in the thermally stabilized test chamber, which guarantees precise measurements. Two generations of the DEPFET sensor PXD5 and PXD6 were tested on the Mini-matrix test system in years 2010-2012 and the results were used for characterization of the sensors and new detector designs.

Electrical characteristics of the DEPFET sensor, the studies of the bulk voltage impact on the charge loss at the edges of the sensor and in-pixel studies on charge collection were investigated using the Mini-matrix test system. Linearity of the DEPFET sensor was proved with pulse width modulated laser and the sensor was calibrated with radioactive sources. DEPFET gated operation was tested on the Mini-matrix system for the first time. DEPFET sensor integrates charge continually in the standard operation. Gated mode of the DEPFET allows making sensor insensitive for incoming radiation for defined time interval. The charge previously stored in the internal gate is saved and integration can continue afterwards. Such fast mechanism which can define a time window, where detector stops integration of new charge, can be used for example to select out noisy bunches injected in an accelerator. This mechanism fundamentally increases scope of applications of the DEPFET sensor and has no parallel in other world pixel sensors.

The measurements of the DEPFET sensors performed on the Mini-matrix test system leaded to unique results and deeper understanding of the DEPFET. Development of extended version of the Mini-matrix system already started and it is expected, that the new version will offer even more detailed measurements of the DEPFET sensors. DEPFET Collaboration is leading to the end of the development of the active pixel detector and the expected start date is in 2015. Development of the Mini-matrix system, test techniques and obtained results are presented in this thesis.

1. CURRENT SITUATION OF THE STUDIED PROBLEM

The theory, which describes the system of known particles and interactions, known as Standard Model [1], [2] and [3], was developed in the second half of 20th century by many physicists. The current formulation was finalized in 1970's and later, it was confirmed by discovery of the bottom quark in 1977, the top quark in 1995, the tau neutrino in 2000 and the Higgs-like boson in 2012. Although the confirmation that properties of the last discovered particle match that of the Standard Model Higgs is still needed, the existence of such a particle strongly supports the validity of the Standard Model. Summary of the Standard Model particles is shown in Figure 1. Beyond the Standard Model still remain many open questions and physicists search for answers as what is the nature of dark matter, unification of forces, how do particles acquire mass and many others. In the last few decades, many groundbreaking physics discoveries were done in high energy physic laboratories as CERN in Switzerland, Fermilab in the USA, KEK in Japan and others. New accelerators and particle physic experiments are planed in the future.

	Fermions			Bosons
Quarks	u up	c charm	t top	γ photon
	d down	s strange	b bottom	Z Z boson
Leptons	ν_e electron neutrino	ν_μ muon neutrino	ν_τ tau neutrino	W W boson
	e electron	μ muon	τ tau	g gluon
	I. generation	II. generation	III. generation	H Higgs boson
				Force carriers

Figure 1 – Elementary Particles of the Standard Model

Belle II experiment [4] plans to confirm the existence of new particles by studies of flavour physics reactions with high statistics. In contrast to Large Hadron Collider (LHC) [5] accelerator at CERN, where protons are accelerated at high energies (up to 2 x 7 TeV) and new particles are studied directly, SuperKEKB is aiming at high statistics allowing indirect studies of new particles. High precision of measurements at Belle II will improve the first results of ATLAS [6] and CMS [7] experiments at CERN.

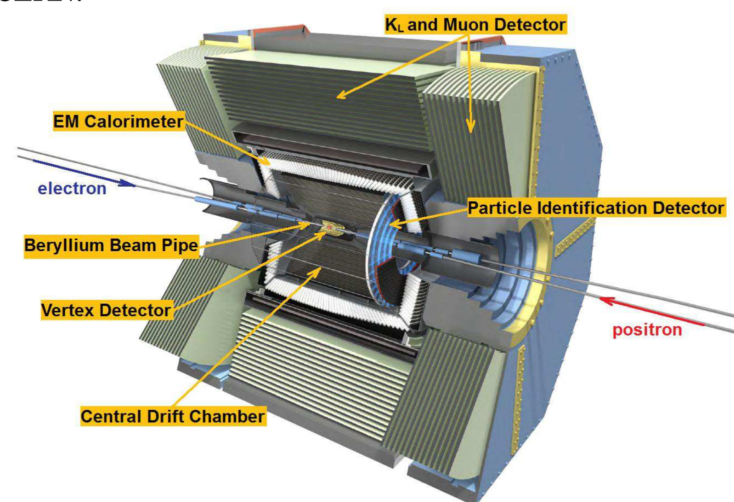

Figure 2 – Belle II Detector [8]

Belle II detector is an upgrade of the previous Belle detector constructed for high luminosity beam. Figure 2 shows schematic drawing of the Belle II detector. Newly generated particles created in collisions of electrons and positrons fly through different detector layers. The vertex detector plays major role in the measurement of B meson decays. The decay time of B meson by weak interaction is extremely short and not possible to measure directly. Hence, the indirect measurement will be carried out by measurement of the decay vertex. The asymmetric beam energies causes shift in the angle of the vertex in the direction of the more energetic electron beam.
The pixel detector makes two innermost layers of the Belle II detector, the first layer with radius 14 mm and the second with radius 22 mm. The inner layer consists of 8 modules and the outer layer of 12 modules. Each module is made of two half-modules, which are glued in the middle. Figure 3 illustrates the arrangement of the pixel detector. The modules are mounted on an integrated support and cooling structure by screws. The support on the backward side can slide on the beam pipe in order to compensate for thermal expansion of the beam pipe and the beam pipe supports.

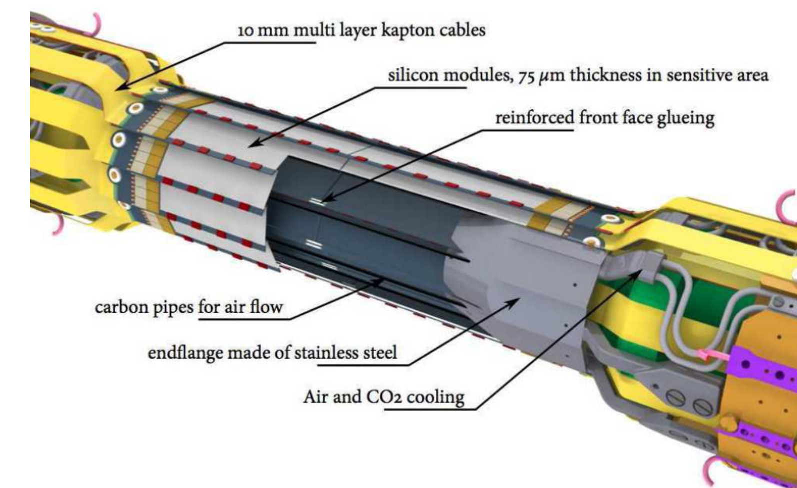

Figure 3 – Pixel Detector [9]

The DEPFET sensor is used for the pixel detector. Very thin sensor can be manufactured due to DEPFETs internal amplification. DEPFET module has 75 µm thickness in the active area. (50 µm thickness of the DEPFET sensor was achieved during the prototyping period.)

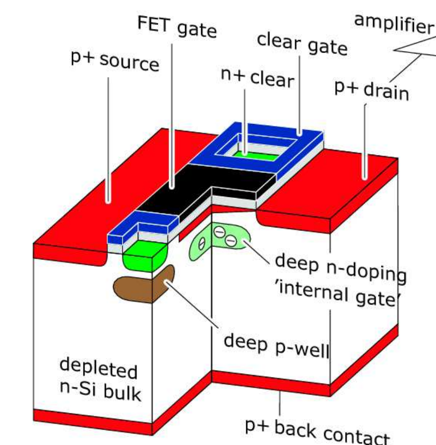

Figure 4 - The DEPFET Operational Principles [9]

A new type of DEPFET pixel detector [10] was proposed by Kemmer and Lutz in 1987. The DEPFET sensor (see Figure 1) consists of a high-resistivity depleted n-substrate and two p-regions, which create a pnp-sandwich structure (p-frontside-implantation, n-substrate, p-backside). Figure 1 illustrates the pixel structure. The n-substrate is depleted sidewards. It means the n-substrate (bulk) is depleted from both sides by applying negative voltages to both p-implantations

with respect to the bulk. The minimum of the electron potential is in a plane parallel to the front surface. Asymmetric depletion voltages are applied to the DEPFET pixel to shift the electron potential minimum close to the front surface, where the MOSFET is located. Additional n-implants hinder electron lateral diffusion and the electrons are concentrated in a small region under the MOSFET channel. This region is called an internal gate. An incoming ionizing radiation generates electron-hole pairs in the depleted n-substrate (bulk), the holes drift to the back-side contact, and the electrons are trapped in the internal gate. The internal gate is located directly under the MOSFET channel below the external FET gate contact, so the charge stored in the internal gate affects the MOSFET channel. New Belle II designs with larger pixels have also drift regions, which ensures homogenous charge collection over the pixel area. When the integration cycle is over, it is necessary to empty the internal gate. This is done by a clear contact next to the MOSFET transistor. The electrons are extracted from the internal gate by applying a high positive voltage to the clear contact. This causes the electrons drift to the clear contact, where they are removed.

Development of the DEPFET pixel detector does not include only sensor itself, but also development of steering and readout electronics, development of test systems and testing, characterization and optimization of the sensor. Various test systems were designed [11], [12], usually based on ASICs (Application Specific Integrated Circuits) primarily designed for the final sensor application. A new system has been developed for testing and characterizing small samples of the DEPFET detector, based on the components of the shelf. The system is an alternative to the steering and readout ASICs [11], [12] and [13]. The system enables precise and low-noise charge measurements and a flexible high resolution configuration of control signals and was used for DEPFET sensor testing.

2. AIMS OF THE DOCTORAL THESIS

The thesis has two major goals which are:

- Development of an alternative precise low-noise test system for the DEPFET prototypes
- Testing and characterization of the DEPFET prototypes on the previously designed test system

Need of a new test system was urged since 2007 in the DEPFET Collaboration by necessity of the ASIC independent system which could handle at least small area of the DEPFET sensor. The primary requirements of the system were following:

- Easy replacement of the tested devices
- Design independent of ASICs
- At least 8 drain channels
- 6 gate and clear channels
- Noise lower than 20 electrons of equivalent noise charge (ENC)
- Universal sequencer and high time resolution configuration of the control sequences (<20 ns)
- Broad amplitude levels of the gate and clear pulses
- Fast design

The requirement of the characterization of the test system itself and its validation is obvious. The basic required measurements on the test system were following:

- Test of basic functionality
- Measurement of electrical characteristics (characterizing) and search for optimal operation point
- Calibration

Other goals have showed up later on, related to the specific DEPFET prototype or accelerator issues. These were:

- Optimization of the drift voltage and in-pixel studies
- Verification of the DEPFET gated mode operation and its quantification

Main benefits of the thesis

Development and construction of the ASIC free high-precision low-noise DEPFET test system (Mini-matrix system) with overall noise around 20 electrons of equivalent input referred noise charge and high-time resolution reconfigurable steering sequences introduced new tool for DEPFET prototyping in the DEPFET Collaboration. The following studies were done on the test system in the frame of this thesis:

- Measurement of the electrical characteristics of the DEPFET sensor and more accurate sensor characterization
- Studies of the impact of the bulk voltage on the charge loss at the edges of the sensor and its optimization
- In-pixel studies of charge collection and optimization of the drift potential in the enlarged pixels. Proof of operation.
- Test of linearity of the DEPFET sensor
- Calibration with radioactive sources
- Proof of concept of operation of the DEPFET in the gated mode
- Study of the charge loss during the gated operation
- Junk charge selection during the blind period of the gated operation

The measurements of the DEPFET sensors performed on the Mini-matrix test system leaded to unique results and deeper understanding of the DEPFET. The gated mode operation of the DEPFET sensor fundamentally increased scope of applications of the sensor and has no parallel in other world pixel sensors and helped to solve the injection noise issue at the SuperKEKB accelerator.

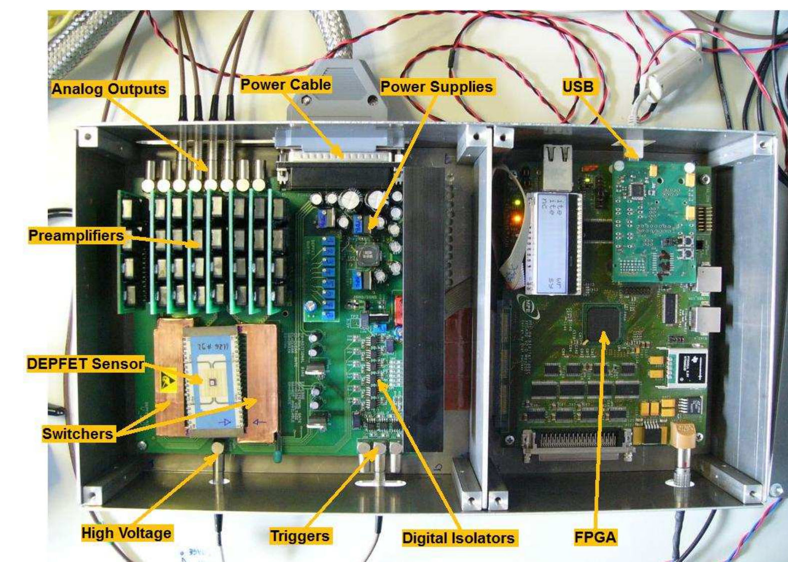

Figure 5 – Photo of the Mini-matrix System

3. WORKING METHODS

A versatile measuring system called Mini-matrix system has been designed to characterize small prototypes of the DEPFET with 48 active pixels. The test system is composed of commercial and custom-made blocks, such as a PC with an 8-channel PCI data acquisition card [14], FPGA (Field-Programmable Gate Array) control card, current readout pre-amplifiers, switching circuit, microprocessor slow control USB card and power supplies. Red or infra red lasers and a 3-axis positioning stage with spatial resolution of 1.25 μm are integrated into the system. The DEPFET sensor is installed in the test chamber equipped with active thermal control system.

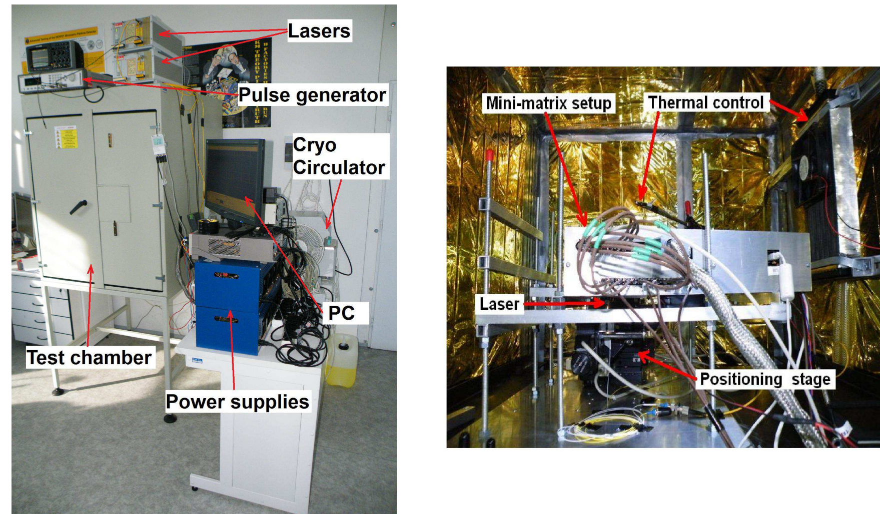

Figure 6 – Left: Configuration of the Measurement Setup. Right: Inside of the Test Chamber

Figure 7 shows a typical digitized stream of the DEPFET matrix drain channel. One pixel is determined by corresponding drain and gate channel. The signal is inverted by preamplifiers, so more negative values means higher signal. Positive spikes in the drain readout stream are caused by clearing pulse. MOSFET channel has capacitive coupling to the clear contact and clear pulse is than visible in the drain signal during the clear process. Switching the gates can also cause spikes in the drain current. These spikes can be efficiently suppressed be adjusting overlaps of gate pulses. The signal of each pixel is evaluated according the following scheme:

1. One row of the pixels is turned on by applying negative voltage at the FET gate.
2. Charge is integrated in the internal gate.
3. Drain current of each transistor in one row is measured in parallel.
4. The whole row is cleared.
5. Drain current is read again.
6. The row is turned off, following row is turned on and the process is repeated.

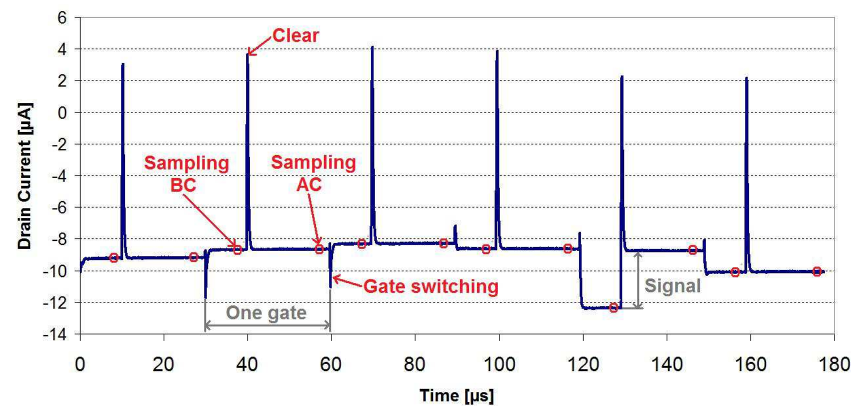

Figure 7 – Drain Current Scope Plot

The signal is evaluated as a difference of currents after clear (AC) and before clear (BC). This readout scheme is called correlated double sampling (CDS) [15]. CDS method is combined with averaging of multiple samples in the Mini-matrix system. This filtering method known as a multi-CDS [16] represents an improvement in compare with traditional RC-CR shapers, widely used in particle physics experiments.

There are several kinds of measurements that may be performed at the Mini-matrix test system. The system was mainly used to test detectors with laser beam or just to evaluate noise of the detector at different operational voltages. Other possibility is usage of the radioactive source.

4. RESULTS

Electrical Characteristics

As a first step of a characterisation of the DEPFET device an optimal voltage operation point has to be found. Source of the MOSFET in the DEPFET pixel is tied to analogue ground AGND and all other DEPFET related voltages are referred to source (AGND). The voltages can be divided in several categories according to the purpose of the voltage and a structure, where it is applied.

MOSFET Related Characteristics

First group of voltages are related to the MOSFETs. These are drain voltage and gate voltage. Gate voltage is clocked and it has two levels: Gate_LOW and Gate_HIGH, which corresponds to on- and off-state of the MOSTET. In the on-state, the MOSFET is operated in saturation region (Gate_LOW < V_{th} , where V_{th} is a threshold voltage). The MOSFET channel is pitched-off and lack of channel region near the drain causes weak dependency of drain current on drain voltage. The drain current is mainly controlled by Gate_LOW voltage and can be modelled approximately as [17]:

$$I_d = \frac{1}{2}\mu_p C_{ox}' \frac{W}{L}\left(V_{gs} - |V_{th}|\right)^2 \left(1 + \lambda V_{ds}\right), \qquad \text{Equation 1}$$

where is μ_p is a charge carrier mobility, C_{ox}' is a sheet capacitance and W and L is a width and length of the gate, λ is a channel-length modulation parameter and V_{ds} is the drain-to-source voltage. The λ parameter is responsible for the differential output resistance of the DEPFET pixel. Output resistance r_{out} can be described as:

$$r_{out} = \frac{\partial V_{ds}}{\partial I_d} = \frac{1}{\lambda V_{ds}}. \qquad \text{Equation 2}$$

Figure 8 shows a measurement of drain current I_d vs. drain-to-source voltage V_{ds}. The Mini-matrix system does not allow measurement of absolute drain current, but only relative changes so the drain current scale is relative only. The differential output resistance of the DEPFET pixel cell is r_{out} = 1.42 MΩ. The drain voltage is set to -5 V.

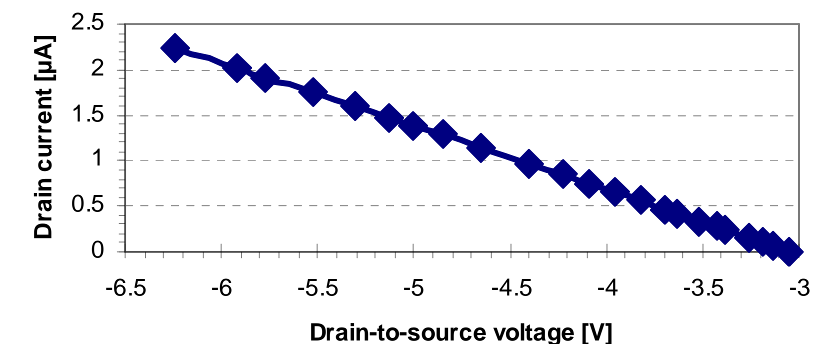

Figure 8 – Drain Current vs. Drain-to-source Voltage

Charge in the internal gate has similar effect on the drain current as a gate voltage change. When charge in the internal gate is present, the Equation 1 can be modified as [18]:

$$I_d = \frac{1}{2}\mu_p C_{ox}' \frac{W}{L}\left(f\frac{q}{C_{ox}} + V_{gs} - |V_{th}|\right)^2 (1+\lambda V_{ds}),$$ Equation 3

where q is the charge in the internal gate, C_{ox} is a capacitance of the gate and f is a reduction factor due to the parasitic coupling of the internal gate. For further calculations the λ can be neglected. According to Lutz [18], when DEPFET is operated in saturation region the transconductance g_m of the DEPFET pixel can by calculated as:

$$g_m = \frac{\partial I_d}{\partial V_{gs}} = -\mu_p C_{ox}' \frac{W}{L}\left(V_{gs} - |V_{th}|\right)^2.$$ Equation 4

Combining Equation 1 (λ is neglected) and Equation 4 results in:

$$g_m = \sqrt{2\mu_p C_{ox}' \frac{W}{L} I_d}.$$ Equation 5

Measurement of drain current vs. Gate_LOW voltage is shown in Figure 9. According to Equation 4 transconductance is calculated: g_m = -26.4 μA/V.
The internal amplification g_q is proportional to the transonductance g_m as:

$$g_q = \frac{g_m}{C_{ox}}.$$ Equation 6

One can see that the value of the g_q is related to the parameters of the MOSFET as L, W, μ_p and C_{ox}'. These parameters are fixed during the design of the sensor and only way how to adjust the g_q during the operation of the sensor is variation of the drain current I_d. Relation between g_q and I_d is approximately:

$$g_q \approx \sqrt{I_d}.$$ Equation 7

Measurements of seed response vs. Gate_LOW voltage of three detector types are shown in Figure 10. The signal charge, generated by laser is constant during the measurement, so the changes of the signal current are caused by variation of the g_q. Since g_q is proportional to the I_d as a square root Figure 10 is in agreement with Equation 7. The Gate_LOW voltage is set to -4 V to achieve highest g_q and reasonably low drain current.

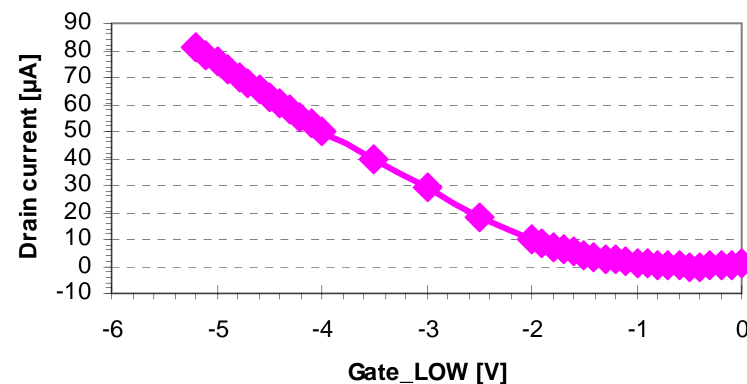

Figure 9 – Pedestal Drain Current vs. Gate_LOW Voltage – PXD6-50µm

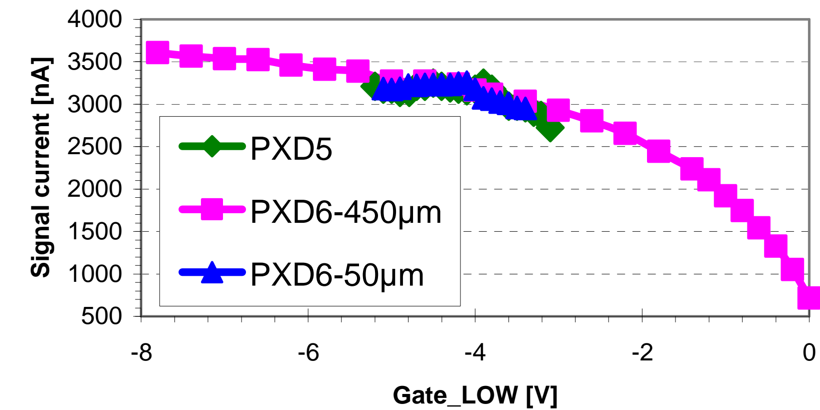

Figure 10 – Seed Response vs. Gate_LOW Voltage

Clear Related Characteristics

Another set of voltages are related to the clearing process and clearing structures. These are Clear_HIGH, Clear_LOW and Clear gate voltages. Clearing performance is important, since noise and signal performance is depending on it. Clear_HIGH voltage is applied to the clear electrode during the clearing process and its amplitude is crucial for complete clear and clearing efficiency of the device. Clearing efficiency of PXD5 and PXD6 detector families can be seen in Figure 11. Inefficient clearing is observed as rising of the pedestal drain current. Due to the reset noise of the correlated double sampling it is necessary to keep clearing efficiency high. The Clear_HIGH voltage is kept around 19 V for all production series.

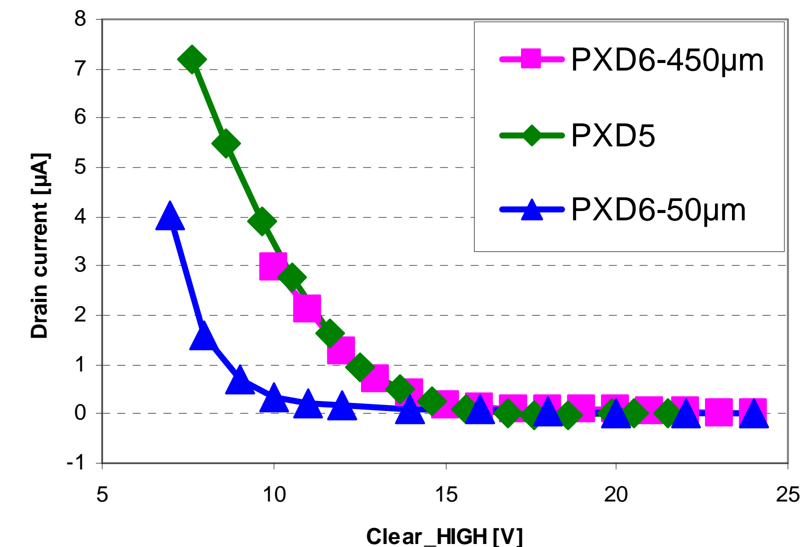

Figure 11 – Clear Efficiency vs. Clear_HIGH Voltage

The Clear_LOW voltage defines base line of the clear pulse. It cannot go too negative, otherwise electrons are back injected from clear contact and integrated in the internal gate. Too high value will cause loosing of electrons from the internal gate during integration and sensor would be continuously cleared. Clear_LOW is kept around 3.8 V. Common clear gate contact is introduced to PXD5 and PXD6 production series. Static clear gate voltage helps to reduce Clear_HIGH voltage and has to be carefully tuned with Clear_LOW voltage. Some parasitic effect can occur at different combinations of Clear_LOW and Common clear gate voltage. These effects are illustrated in Figure 12, where both voltages were swept in 3D plot.

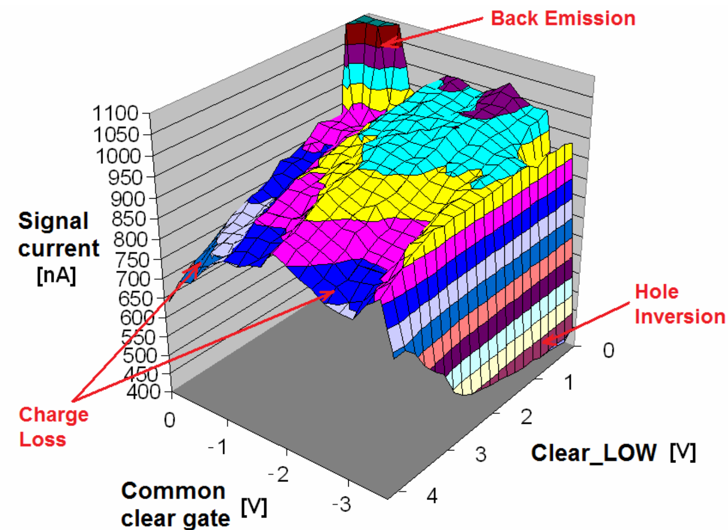

Figure 12 – Seed Response vs. Gate_LOW and Common Clear Gate Voltage of PXD5 Detector

Following parasitic effects were observed:

1. Back Emission: Electrons are emitted from the clear implantation and integrated in the internal gate, when Clear_LOW voltage is too low. Back electron emission leads to detector saturation.
2. Charge loss: Too high Clear_LOW voltage causes continuous clearing and lost of charge from the internal gate. Too positive common clear gate voltage causes accumulation of electrons under the clear gate contact which will not reach the internal gate and will be lost during the clearing cycle.
3. Hole inversion: When the clear gate voltage is too negative a p-channel can develop in the n-bulk under the clear gate contact. This channel can short drain and source or source and clear p-well and will disable sensor operation.

Other Characteristics

The remaining set of voltages is bias back depletion voltage, bulk voltage and drift voltage. Bulk voltage will be discussed in the following chapter separately. Drift voltage is introduced only to the PXD6 detector families and will be discussed later too. Depletion voltage is connected to the back contact and it is depleting back side of the detector. Figure 13 shows a measurement of a seed charge versus back depletion voltage. A sharp threshold is visible in measured plots. Detector is not fully depleted below threshold voltage and it is not sensitive for light. Since voltage measurements were done with the red laser, charge is generated only at the back surface of the detector and full depletion is necessary for signal detection. 450 µm thick detectors are fully depleted around -120 V. 50 µm thick detector is fully depleted around -21 V.

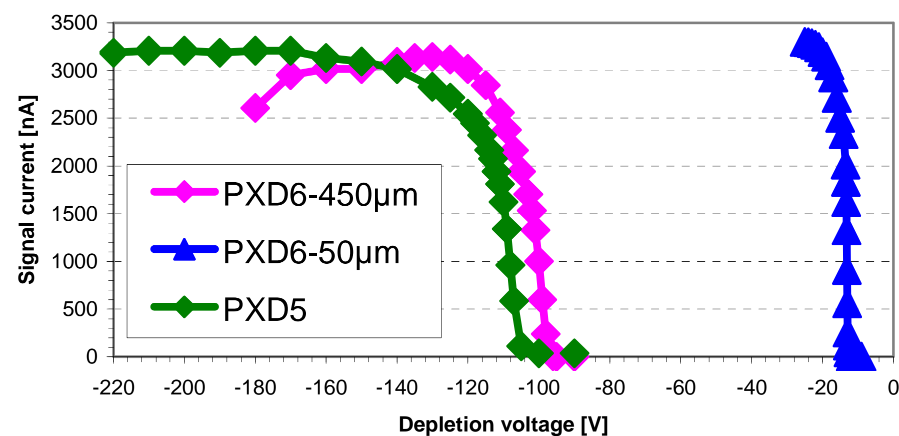

Figure 13 – Seed Response vs. Back Depletion Voltage

Edge Effect

Pixels, which are located at the edges of the detector, might suffer by lost of charge, which escapes to bulk and surrounding edge structures. The Mini-matrix system usually does not use whole area of the detector, so at some detector samples the edges of the detector are not accessible (all PXD6). PXD5 mini-matrices tested at the system allow access to two edges of the detector. Direction in x axe is row-wise. Direction in z axe is column-wise. First and last rows are the edges of the detector and that first and last two rows are affected by the edges of the detector. Variation of the bulk voltage improves charge loss at the edges. Bulk voltage contact is located at the outer ring of the sensor. Bulk voltage has to be positive with respect to source otherwise bulk-source PN junction become polarized forward and current is injected from bulk to MOSFET channel. Figure 14 presents a set of 2D laser scans with cluster charge maps for various bulk voltages.
When bulk voltage is rather positive, electrons generated at the edge of the detector by laser are attracted by bulk ring and edge pixels become insensitive. Beginning of bulk current injection is visible, when bulk voltage is 0.5 V. Pixels, where bulk current injection occurs are completely saturated and read as zero. Optimal bulk voltage was found at 2 V. Additional edge rings were placed at some DEPFET prototypes, which gives more space for optimization, but these rings were not connected in the Mini-matrix system.

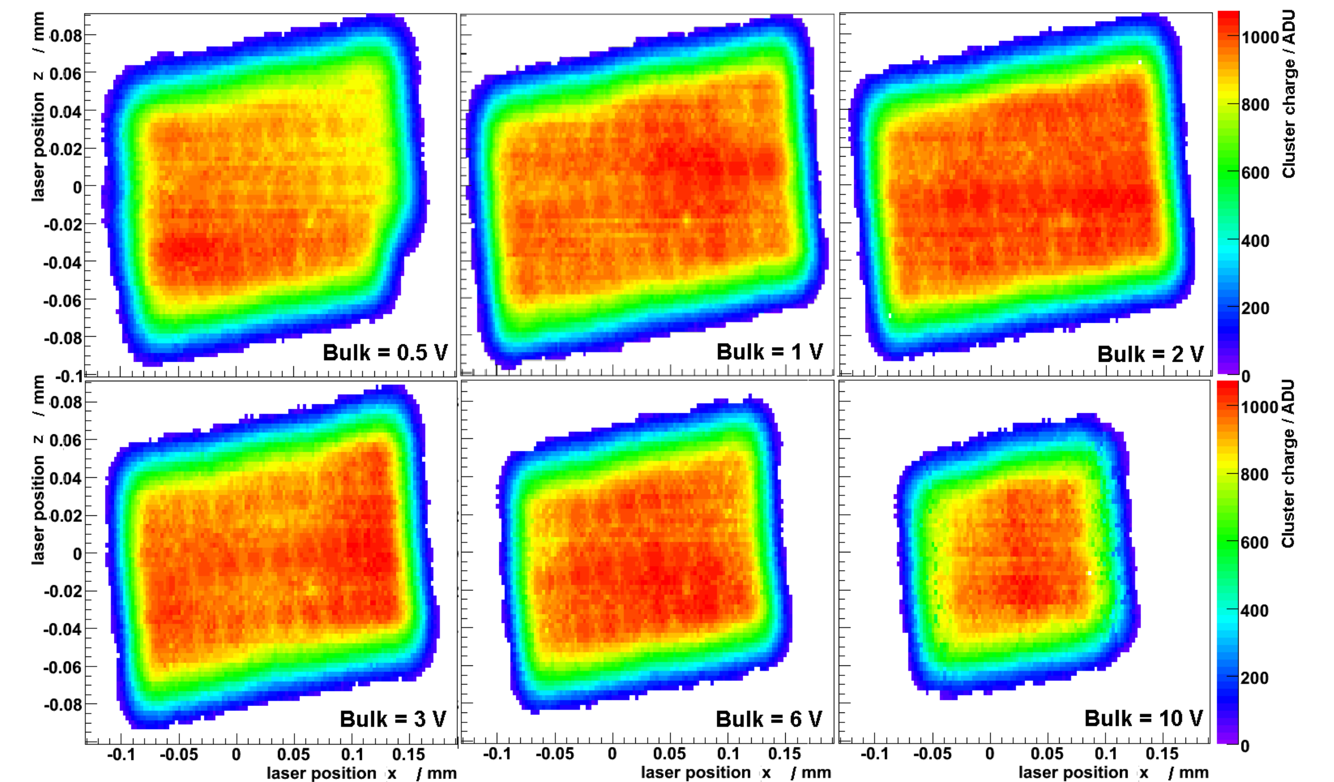

Figure 14 – Cluster Charge vs. Laser Position

Drift Regions

The Belle II design PXD6 matrices which have drift regions added to the larger pixels have additional drift voltage which has to be optimized. It improves drift of electrons from the area of the enlarged pixel. The voltage applied to the drift regions has strong effect on the charge collection of the detector. Too positive drift voltage causes inefficient charge collection. Poor charge collection was observed for higher drift voltages than -1 V. It is caused by low lateral electrical field in the pixel and very slow electron drift to the internal gate. When the electrons do not reach the internal gate in the integration time, the clear cycle is performed and the charge is lost. Figure 15 presents a set of 2D cluster charge measurements for different drift voltages. When the drift voltage is close to 0 V, charge collection is poor in regions more remote from the centres of the quadruple pixels with common gate electrodes. Black contours show the measurement of seed charge collection at optimal operational voltages. It indicates the centres of the pixels. The charge collection is

homogeneous for drift voltage higher than 1 V. More negative drift voltage negatively affects gain of the detector. Drift voltage was set to -2 V.

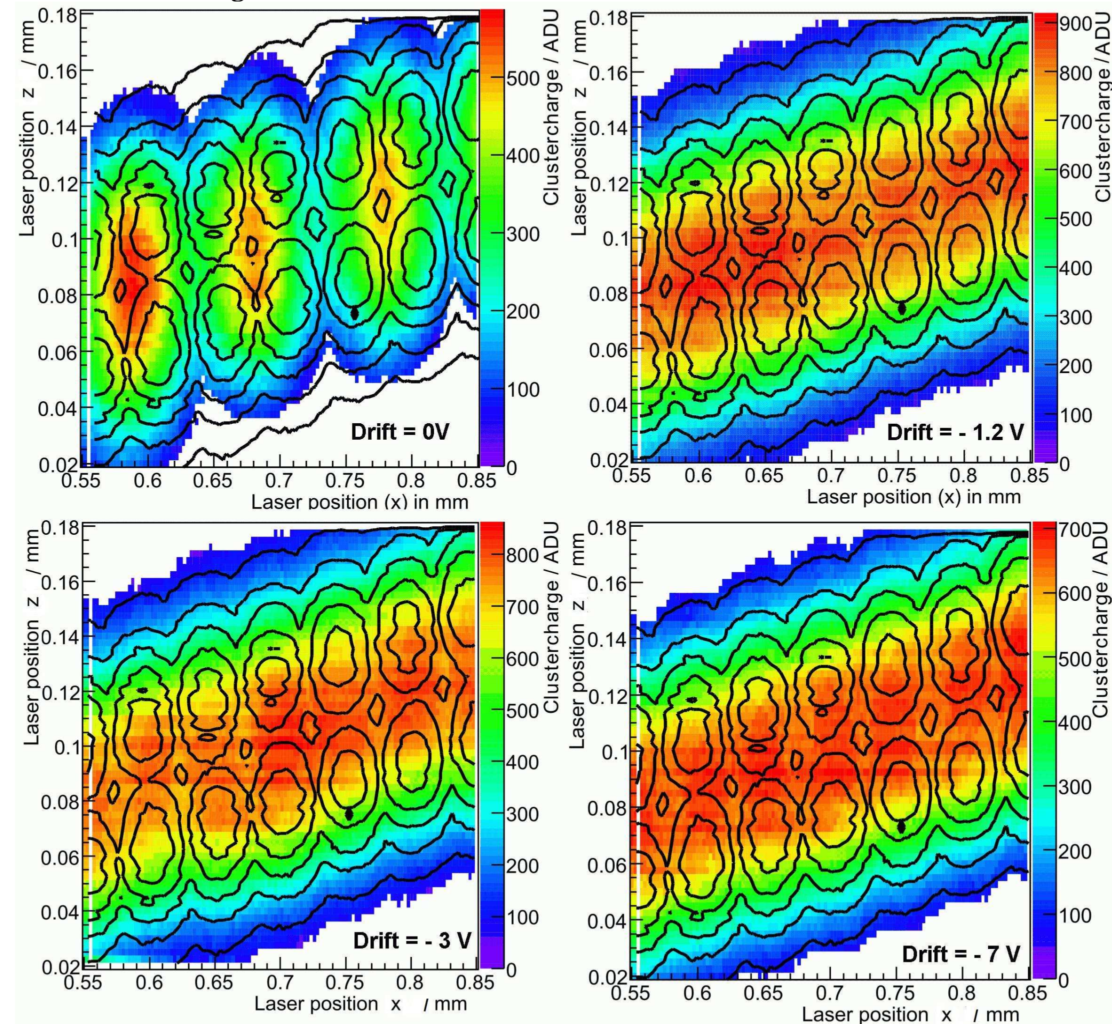

Figure 15 – Cluster Charge vs. Laser Position

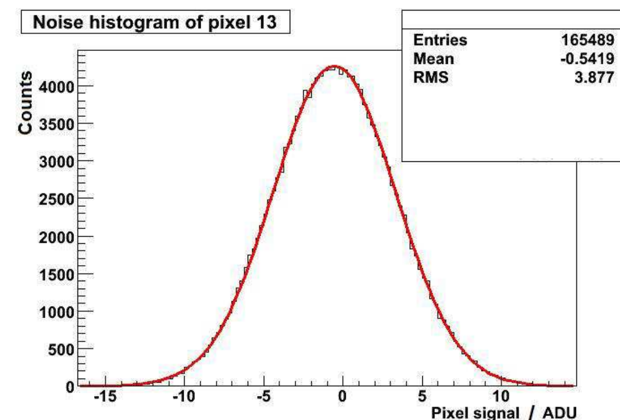

Figure 16 – Noise Histogram of Pedestals

System Noise

The noise of the DEPFET detector and DEPFET sensor itself are closely tied together. The overall noise value is given by intrinsic noise of the DEPFET sensor, noise of all amplifiers in the signal way, but also by noise of the power supplies and voltage regulators and noise of the pulse generators. It would be difficult to separate these noise sources and measure noise contribution of each of them. So the system noise was measured which defines noise of the DEPFET Mini-matrix

system including all electronic subsystems. The system noise also depends on the timing of the steering sequences and averaging and correlated double sampling adjustment. Figure 16 shows a noise histogram of one pixel pedestals of the PXD6 DEPFET matrix. RMS noise 3.9 ADU corresponds to 7 nA of equivalent input referred noise current or 20 electrons of equivalent noise charge. The noise levels vary in range of ± 1 ADU for different pixels. The comparable values were achieved also for PXD5 generation sensors.

DEPFET Linearity

The relation between drain current I_d and charge in the internal gate q is linear when MOSFET in the DEPFET pixel is operated in saturation mode. In the Mini-matrix system, the laser is used in pulsed operation mode where short laser pulses are applied to the DEPFET sensor during each integration cycle. Adjustment of the optical laser power can be easily done by variation of the laser pulse width. When we assume, that the temperature of the laser module is constant (mean input power is in the level of μW) than output optical power is proportional to the laser pulse width. The measurement of the DEPFET linearity was proven on the Mini-matrix system.

Calibration

Detector calibration was done by x-ray sources with discrete energy peaks. Photons with energies lower than 100 keV are absorbed in silicon via photo effect. Their complete energy is converted to generation of electron-hole pairs. Energy necessary for generation of one electron-hole pair is $E_{e\text{-}h}$ = 3.65 eV. The number of generated electron-hole pairs n can be calculated as:

$$n = \frac{E_\gamma}{E_{e-h}}, \qquad \text{Equation 8}$$

where E_γ is energy of absorbed photon.

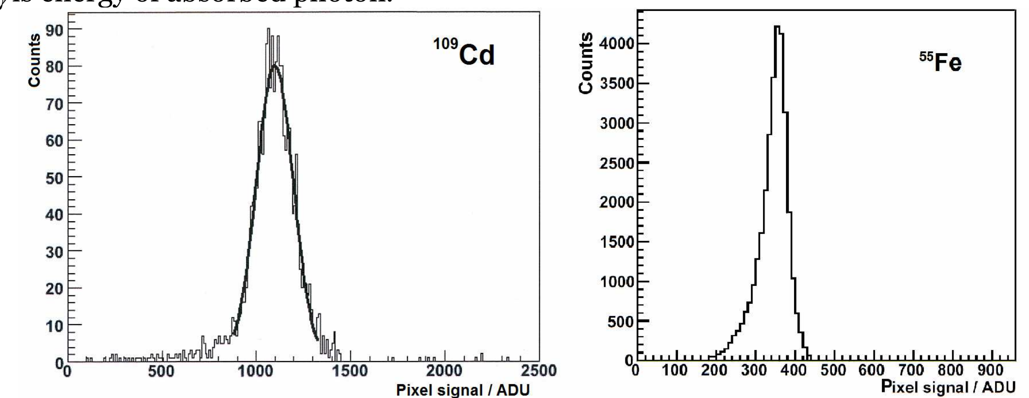

Figure 17 – Spectra of the Radioactive Sources

Figure 17 presents spectra obtained by irradiation of the PXD5 generation detector with a ^{55}Fe source (5.9 keV) and ^{109}Cd source (22 keV), measured at the Mini-matrix system in the MPI Munich. Internal amplification of the DEPFET pixels, g_q can be calculated when ADU is calibrated in the scale of pA. The calculated internal amplification is in range 368 - 457 pA/e$^-$. Comparable results can be found in [11], [9] and [19]. The PXD6 generation detector was not calibrated with the radioactive sources at the Mini-matrix system due to the layout with 2 x 24 active pixels. PXD6, was calibrated using the red laser and approximately internal amplification 340 pA/e$^-$ was measured.

DEPFET Gated Operation

Gating the DEPFET is a unique function of the detector which allows making sensor insensitive for incoming radiation for defined time interval. The charge previously stored in the internal gate is saved and integration can continue afterwards. This operation stage is achieved by applying Gate_High (OFF) and Clear_High (ON) voltages in the same time. In contrast to the real clear,

when Gate_Low (ON) voltage is applied during the clearing and electrons can escape from the internal gate by thermoionic emission, during the suppressed clear a potential barrier for electrons in the internal gate is formed and electrons cannot be cleared. The potential of the internal gate is shifted by a capacitive coupling to the external gate electrode. The Clear_High (ON) voltage applied during the insensitive (blind) period creates a shielding potential which deflects trajectories of newly generated electrons and they are extracted to the clear electrode.

Charge Loss Measurement

The gated mode operation introduces additional clear pulse to the steering sequence. This pulse might cause additional loses of charge in the internal gate. Therefore, measurement which determines charge losses due to the additional shielding clear pulse was carried out. In this test, charge was generated during the integration time, before the shielding clear pulse. Difference of charge stored in the internal gate with and without the shielding clear pulse versus generated charge was measured in Figure 18. The measurement was performed with the red (660 nm) laser. Number of electrons lost due to the shielding clear pulse increases with charge in the internal gate and saturates around 200 electrons. The length of the clear pulse in the insensitive mode was set to 4.8 μs as a nominal value. Impact of the clear pulse width to charge loss was measured, but no significant effect was observed within the error of the measurement.

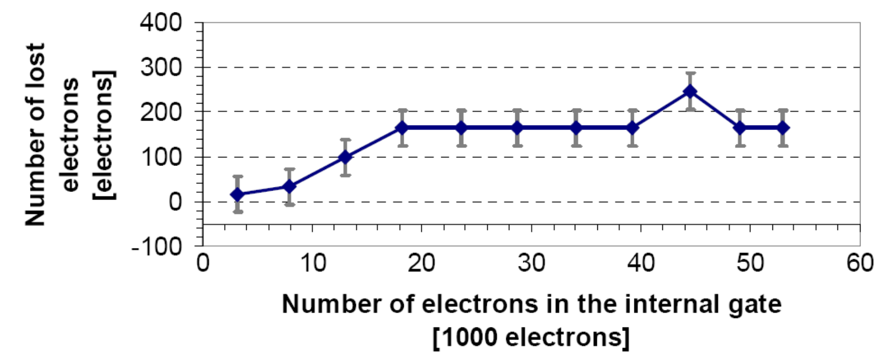

Figure 18 – Charge Loss Due to the Shielding Clear Pulse vs. Charge in the Internal Gate

Charge loss from the internal gate is affected by setting of the operational voltages. The critical voltage is Gate_High voltage, which couples electrons in the internal gate during the blind mode operation. When the external gate voltage is set more negative, internal gate is moving deeper under the surface of the external gate and the capacitive coupling becoming weaker and for voltages lower than 3.5 V electrons start loosing from internal gate as visible in Figure 19. Charge loss dependence due to the additional shielding clear pulse as well as dependence on Back, Clear Gate and Clear_High voltages was also measured, but no tendencies within the error of measurement were observed.

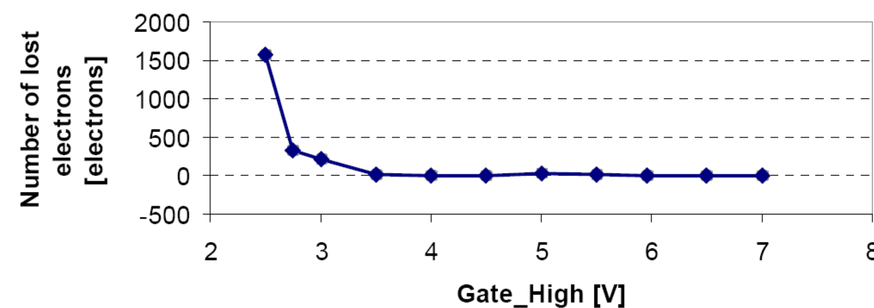

Figure 19 – Charge Loss Due to the Shielding Clear Pulse vs. Gate_High Voltage

Junk Charge Selectivity

When the DEPFET is switched into the insensitive (blind) mode, charge generated during this period (junk charge) goes directly to the clear electrode. Small fraction of the generated charge gets anyway into the internal gate. This effect is called junk charge selectivity. For measurement of junk charge selectivity, charge was generated by laser only during the insensitive mode. Figure 20, left displays surface scan with the infrared laser (1060 nm) of the 450 μm thick matrix. The infrared laser beam penetrates through full thickness of the sensor, hence, sharp increase of junk charge selection is observed when the beam hits the internal gate and part of the charge is generated in the internal gate. Six red points corresponds to six pixel's internal gates. Figure 20, rights displays zoom of one pixel. The junk charge selection is affected by settings of operational voltages and some of them have important role in optimization. Clear_High voltage, which creates shielding potential, decreases junk charge selectivity when is set more positive (see Figure 21). This effect can be explained by higher electrical fields in the bulk structure and higher drift of junk electrons to the clear electrode. Higher Clear_High voltage also increases clear efficiency, as discussed in upper, but clear voltage cannot be chosen too positive due to the system issues.
Another voltage, which influences the junk charge selectivity, is the back voltage. Setting with more positive values decreases selection of junk charge. Explanation can be found in lower reach of shielding clear potential as well as lower sensitivity of depleted bulk for charge generation.

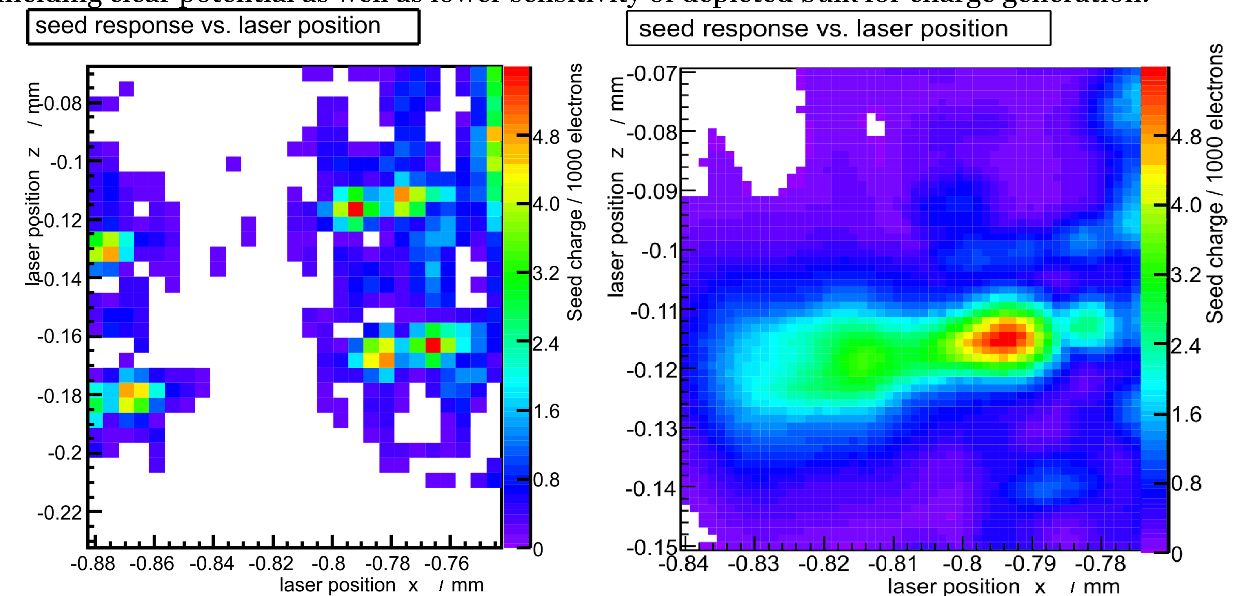

Figure 20 – Surface IR Laser Scan of the PXD6 450 μm Thick Detector
LEFT: 6 Pixels, RIGHT: 1 Pixel

There was observed strong affection of junk charge selection by clear gate voltage, when clear gate voltage was set close to the positive values. But it has to be kept in mind that n-channel starts forming in the clear p-well for positive clear gate voltages and low junk charge selection is mainly result of the charge loss from the internal gate.

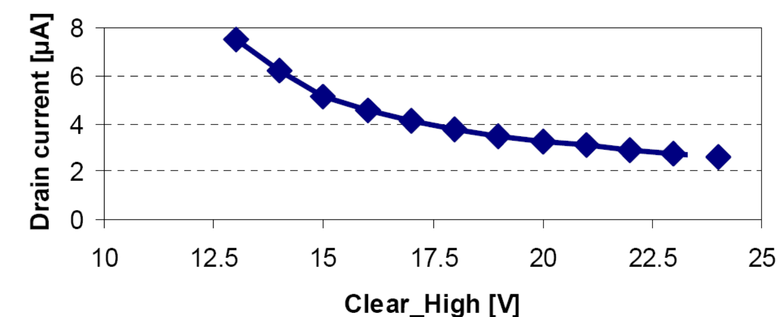

Figure 21 – Junk Charge Selectivity vs. Clear_High Voltage

Figure 22 compares surface red laser scans maxima (seeds) of junk charge selection and standard signal selection. The junk charge selection maxima are approximately 10 µm shifted inwards in compare with centres of seeds for normal operation. This is caused by low junk charge collection in the drift regions of the matrix, which shifts seeds centres closer to the internal gate. During the standard operation the charge collection is homogeneous over whole pixel are, hence seed centre is in the middle of the pixel. This observation leads to conclusion, that for the worst case scenario, single point measurements should be done over the internal gate location.

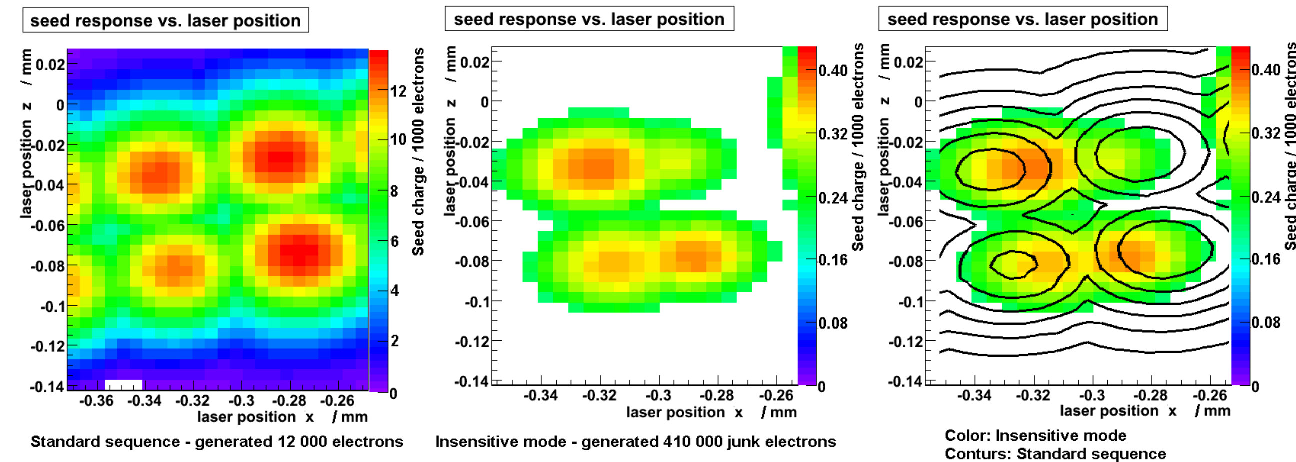

Figure 22 – Surface Red Laser Scan of the PXD6 450 µm Thick Detector

In the worst case scenario, incoming particle goes through the area of the internal gate, leaving fraction of the generated junk charge in the internal gate. Figure 23 shows results of a single point measurement, when the infrared laser points directly to the internal gate for different sensor thicknesses and operational voltages. Such measurement imitates the worst case scenario when the most sensitive part of the detector for junk charge selection is evaluated. The settings called “Optimal” give low junk charge selectivity and the signal selection is not deteriorated, but the final system limitation is not taken into account. A fraction of captured electrons of the junk charge generation is more less constant with number of generated electrons. Fractions of captured junk charge were measured in Table 1.

Table 1 – Junk Charge Selection

Detector	Thickness [µm]	Pixel Size [µm x µm]	Voltage Settings	Junk Charge Selection [%]
PXD6	450	50 x 50	Nominal	3.6
PXD6	450	50 x 50	Optimal	1.6
PXD6	50	50 x 50	Nominal	4.3
PXD6	50	50 x 50	Optimal	3.5

Lower junk charge selection of the thick detector is given by the geometrical distribution of the detector volume, which is shielded against the junk charge and the volume near to the internal gate, where generated junk charge is captured. The layout of thick and thinned detectors is identical, as well as the depth of the internal gate. Hence, the volume sensitive for the junk charge is similar for the thick, as well as for the thinned detector. On the other hand, the thinned detector has much thinner bulk region, where shielding against junk charge is effective. Average junk charge selection over whole area of the sensor is calculated in the following chapter.

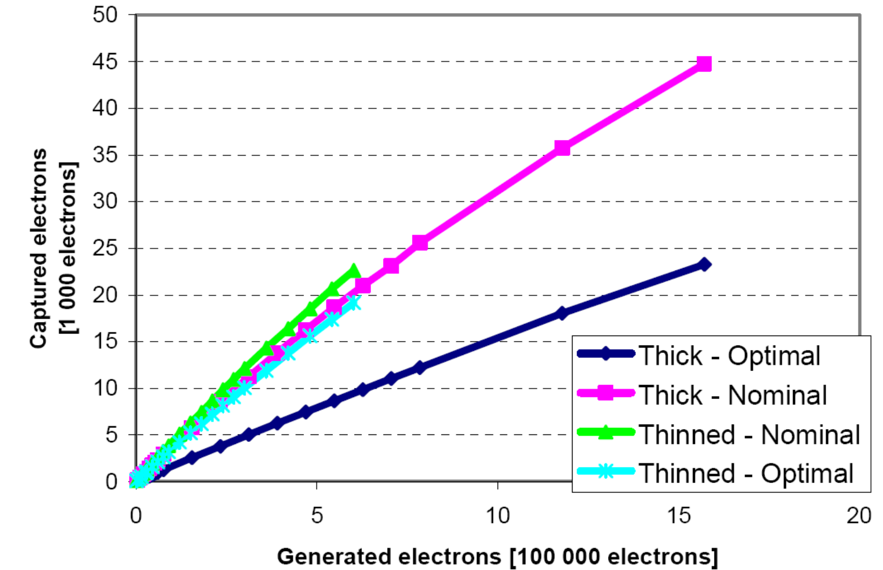

Figure 23 – Single Point Junk Charge Selection vs. Generated Junk Charge

Average Junk Charge Selection

The values of junk charge selection calculated in the previous chapter show the worst case, when the infrared laser beam (or incoming particle) hits the internal gate, where the sensor is the most sensitive. This region is rather small in compare with overall pixel area. Figure 24, left demonstrates spatial junk charge sensitivity of the PXD6 thinned matrix with nominal voltage settings. Figure 24, right than highlights regions, where junk charge selectivity is higher than 2 % of generated junk charge. Estimation of average junk charge selection can be done, when the pixel area (50 µm x 50 µm) is divided into two regions, where junk charge selection is lower than 2 % and the region, where it is more than 2 %. The sensitive region makes approximately 8 % of overall pixel area. When we assume that there is 4.3 % junk charge selection in the sensitive area and 0 % over the rest of the pixel the average junk charge selection over the pixel area is 0.34 %.

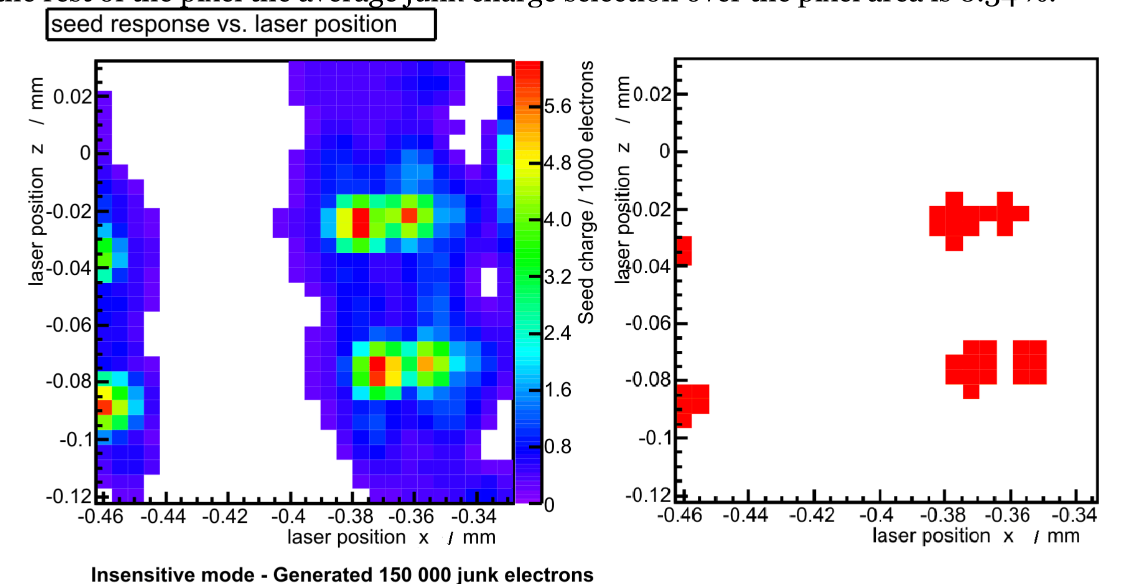

Insensitive mode - Generated 150 000 junk electrons

Figure 24 – Surface IR Laser Scan of the PXD6 50 µm Thick Detector
LEFT: Seed Response, RIGHT: Junk Charge Selectivity > 2 %

The estimation can be done also for the bigger pixels used in the vertex detector. The bigger pixels (50 µm x 70 µm) have only bigger drift regions. MOSFET structure as well as the internal gate stays the same, so we can assume that the sensitive area will be the same and the ratio of sensitive over non-sensitive area will decrease.

Table 2 – Average Junk Charge Selection (* Extrapolated values)

Detector	Thickness [μm]	Pixel Size [μm x μm]	Average Junk Charge Selection [%]
PXD6	450	50 x 50	0.29
PXD6	50	50 x 50	0.34
PXD6*	50	50 x 70	0.28

5. CONCLUSION

New type of the pixel detector DEPFET is being developed for the Belle II detector at electron-positron SuperKEKB collider in Japan and future International Linear Collider. The DEPFET sensor introduces new concept of active pixels with low noise at room temperature, non-destructive repetitive readout and thinned technologies. The pixel detector for Belle II consists of two cylindrical layers arranger around the beam pipe.

The DEPFET test system called Mini-matrix system was designed for testing and characterization of small DEPFET prototypes. The system has overall noise around 20 electrons of equivalent noise charge and repeatability of the measurement is within the same error. It can drive sensors with 48 active pixels and the steering sequences are reconfigurable with high time resolution of 7.5 ns. The test system integrates a computer controlled positioning of a laser beam focuser which can scan the detector surface with high resolution of 1.25 μm and computer controlled power supplies, so automated tests can be performed. The system is placed in the thermally stabilized test chamber with stability of 0.1 °C, which guarantees precise measurements. The achieved parameters of the system and test techniques has lower noise, higher spatial resolution and precision than systems based on ASICs primarily designed for final application described in [11] and [12]. The measurements of the DEPFET sensor performed on the Mini-matrix test system leaded to unique results and deeper understanding of the DEPFET and were published in refereed journals. Several versions of the test system were designed and some pieces of the test systems were supplied to other laboratories.

The DEPFET samples tested on the system had various layouts and thicknesses (450 μm and 50 μm) as the development of the pixel detector was heading to the final design. Two generations of the DEPFET sensor PXD5 and PXD6 were tested on the Mini-matrix test system and the results were used for characterization of the sensor and new detector designs.

Electrical characteristics of the DEPFET sensor were investigated using the Mini-matrix test system. Optimal operational point of the MOSFET cell was found and the differential output resistance of the DEPFET pixel cell r_{out} = 1.42 MΩ and transconductance g_m = -26.4 μA/V were determined. Clear performance of the DEPFET sensor was investigated and it was found, that Clear_HIGH voltage has to be higher than 15 V to achieve complete clear of the internal gate for 450 μm thick sensors. Sensors with thickness 50 μm required only 12 V for complete clear. Higher values are recommended. Combination of Clear_LOW and Common Clear Gate voltage helps to reduce clear voltage swing, but parasitic effects can occur when wrong combination of these voltages is set. DEPFET sensor works in full depletion so appropriate back depletion voltage has to be supplied to achieve correct operation. For 450 μm thick sensors the depletion voltage has to be higher than 120 V. For 50 μm thick sensors the full depletion was observed at voltages higher than 21 V. Comparable results can be found in [11] and [12], but also new PXD6 DEPFET prototypes wave been investigated in this thesis.

The edges of the sensor introduce risk of charge loss into the bulk of the sensor or back injection of charge from balk. The studies of the bulk voltage were carried out and the optimal bulk voltage 2V was found.

The Belle II design PXD6 matrices have new drift regions added to the enlarged pixels. It improves drift of electrons from the more remote area of the pixel. The voltage applied to the drift regions has strong effect on the charge collection of the detector. The in-pixel studies on charge collection were done and it was found that too positive values of the drift voltage leads to charge lost from more remote areas of the pixels. Optimal drift voltage -2 V was found. These results have not been published yet.

Linearity of the DEPFET sensor was proven with pulse width modulated laser and the sensor was calibrated with radioactive sources. Internal amplification of PXD5 generation matrix was measured in range 368 - 457 pA/e^-. Internal amplification of PXD6 generation matrix was derived from PXD6 by using laser beam as approximately 340 pA/e^-. Comparable results achieved with radioactive sources have been presented in [19]. Suitability of the pulsed laser beam for precise detectors tests has been shown.

DEPFET gated operation was tested on the Mini-matrix system. This operation allows making sensor insensitive for incoming radiation for defined time interval. The charge previously stored in the internal gate is saved and integration can continue afterwards. This operation stage is achieved by applying positive voltage at the MOSFET gate electrode and positive voltage at the clear contact in the same time. The positive clear voltage applied during the insensitive period creates a shielding potential which deflects trajectories of newly generated electrons and they are extracted to the clear electrode. Such fast mechanism which can define a time window, where detector stops integration of new charge, can be used for example to select out noisy bunches injected in an accelerator. To prove this concept of operation, measurements with red and infra red laser were carried out on the DEPFET Mini-matrix system. It was proven, that DEPFET can operate in this way. The average charge selection in the insensitive mode is lower than 0.4% and the suppressed clear mechanism does not cause charge loss higher than 200 electrons. Flexibility of the Mini-matrix system, precision and long term stability leaded to the results which have not been published yet and could not been obtained on other previous test system based on ASICs.

Development of extended version of the Mini-matrix system already started and it is expected, that the new version will offer even more detailed measurements of the DEPFET sensors. DEPFET Collaboration is leading to the end of the development of the active pixel detector and the expected start date is in 2015.

List of literature used in the thesis statement

[1] GLASHOW, S. L.: *Partial Symmetries of Weak Interactions*, Nucl. Phys. 22 579, 1961

[2] WEINBERG, S.: *A Model of Leptons*, Phys. Rev. Lett. 19 1264, 1967

[3] SALAM A.: *Weak and Electromagnetic Interactions*, In the Proceedings of 8th Nobel Symposium, Lerum, Sweden, pp 367-377, 1968

[4] DOLEZAL, Z., UNO, S., et al.: *Belle II Technical Design Report*, KEK Report 2010-1, 2010

[5] Home Page of the LHC: http://lhc.web.cern.ch/lhc

[6] Home Page of the ATLAS Experiment: http://www.atlas.ch

[7] Home Page of the CMS Experiment: http://cms.web.cern.ch

[8] Belle II Experiment Home Page: http://belle2.kek.jp

[9] DOLEZAL, Z., KIESLING, C., LACASTA, C., MOSER H.-G. et al.: *The Belle II PXD Whitebook*, DEPFET Collaboration, 2012

[10] KEMMER, J., LUTZ, G.: *New Detector Concepts,* Nuclear Instruments and Methods in Physics Research A253 365-377, 1987

[11] TRIMPL, M.: *Design of a Current Based Readout Chip and Development of DEPFET Pixel Prototype System for the ILC Vertex Detector, PhD Thesis,* Bonn University, 2005

[12] KOCH, M.: *Development of a Test Environment for the Characterization of the Current Digitizer Chip DCD2 and the DEPFET Pixel System for the Belle II Experiment at SuperKEKB*, *PhD Thesis,* Bonn University, 2011

[13] FISCHER, P., PERC, I., GIESEN, F., KREIDL, C.: *Switcher 3 Reference Manual*, Mannheim University, 2007

[14] *Octopus CompuScope 83XX - 14-Bit Family of Multi-channel Digitizers for the PCI Bus Datasheet*, www.gage-applied.com, 2006

[15] WHITE, W. H., LAMPE, D. R., BLAHA, F. C., MACK, I. A. *Characterization of surface channel CCD image arrays at low light levels*, IEEE Journal of Solid-State Circuits Vol.SC-9, pp.1-14, 1974

[16] BUTTLER, W., HOSTICKA, B.J., LUTZ, G.: *Noise Filtering for Readout Electronics*, Nuclear Instruments and Methods in Physics Research A288 187-190, 1990

[17] TSIVIDIS, Y.: *Operation and Modeling of the MOS Transistor*, Oxford University Press, 1999

[18] LUTZ, G.: *Semiconductor Radiation Detectors*, Springer Verlag, Berlin, 1999

[19] RUMMEL, S., ANDRICEK, L., MOSER, H.-G., RICHTER R. et al.: *Intrinsic Properties of DEPFET Active Pixel Sensors*, Journal of Instrumentation, 2008

List of candidate’s works relating to the doctoral thesis

Impacted Publications on Web of Science

[A1] ANDRICEK, L., KODYŠ, P., KOFFMANE, C., NINKOVIC, J., OSWALD, C., RICHTER, R., RITTER, A., RUMMEL, S., **SCHEIRICH, J**.*, WASSATSCH, A.: *Advanced Testing of the DEPFET Minimatrix Particle Detector*, Journal of Instrumentation, 2012 (Impact Factor 2011 = 1.869)

[A2] ANDRICEK, L., CARIDE, J., DOLEŽAL, Z., DRÁSAL, Z., ESCH, S., FREY, A., FURLETOVA, J., FURLETOV, S., GEISLER, C., HEINDL, S., IGLESIAS, C., KNOPF, J., KOCH, M., **KODYŠ, P.***, KOFFMANE, C., KREIDL, C., KRÜGER, H., KVASNIČKA, P., LACASTA, C., MALINA, L., MARIÑAS, C., NINKOVIC, J., REUEN, L., RICHTER, R. H., RUMMEL, S., SCHEIRICH, J., SCHNEIDER, J., SCHWENKER, B., VÁZQUEZ, P., VOS, M., WEILER, T., WERMES, N.: *Intrinsic resolutions of DEPFET detector prototypes measured at beam tests*, Nuclear Instruments and Methods in Physics Research A, 2011 (Impact Factor 2011 = 1.207)

[A3] **URBÁŘ, J.***, SCHEIRICH, J., JAKUBEK, J.: *Medipix/Timepix cosmic ray tracking on BEXUS stratospheric balloon flights*, Nuclear Instruments and Methods in Physics Research A, 2011 (Impact Factor 2011 = 1.207)

Refereed Scientific Journals

[A4] **SCHEIRICH, J.***: *The DEPFET Mini-matrix Particle Detector*, Acta Polytechnica, ČVUT Press, Praha, 2010

Other Publications

[A5] **SCHEIRICH, J**.*, OSWALD, C., KODYŠ, P.: *First measurement on the DEPFET Mini-matrix particle detector system*, ASDAM, IEEE, 2010

[A6] **URBÁŘ J.***, SCHEIRICH J., JAKŮBEK J.: *MEDIPIX Cosmic Ray Tracking Device on BEXUS-7 Stratospheric Balloon Flight*, Proceeding of the 19th ESA Symposium on European Rocket and Ballon Programes and Related Research, European Space Agency, Noordwijk NL, 2009

[A7] **SCHEIRICH, J.***: *DEPFET Mini-matrix Particle Detektor*, POSTER 2010 - Proceedings of the 14th International Conference on Electrical Engineering, CTU in Prague, FEE, 2010

[A8] **VOS, M.***, FUSTER, J., LACASTA, C., MARINAS, C., DIEGUEZ, A., GARRIDO, L., GASCON, D., COMERMA, A., FREIXES, L., CASANOVA, R., VILELLA, E., RIERA-BABUES, J., VILASIS-CARDONA, X., GASPAR, A., PAJARES, J., RODRIGUEZ, P., FURLETOVA, J., FURLETOV, S., KOHRS, R., KOCH, M., KRÜGER, H., REUEN, L., SCHNEIDER, J., WERMES, N., FISCHER, P., KREIDL, C., PERIC, I., KNOPF, J., LANGE, S., KÜHN, W., MÜNCHOW, D., FREY, A., GEISLER, C., SCHWENKER, B., DE BOER, W., BARVICH, T., BROVCHENKO, O., HEINDL, S., SIMONIS, H.J., WEILER, T., BRODZICKA, J., BOZEK, A., KAPUSTA, P., PALKA, H., ANDRICEK, L., CHEKELIAN, V., KIESLING, C., KOFFMANE, C., LU, S., LUTZ, G., MOLL, A., MOSER, H.G., NEDELKOVSKA, E., NINKOVIC, J., PROTHMAN, K., RICHTER, R., RITTER, M., RUMMEL, S., SIMON, F., DOLEZAL, Z., DRASAL, Z., KODYS, P., KVASNICKA, P., SCHEIRICH, J., CARIDE, J., ESPERANTE, D., GALLAS, A., PEREZ, E., RODRIGUEZ, P. VAZQUEZ, P.: *DEPFET active pixel detectors*, Proceedings of Science, 2009

Technical Reports

[A9] DOLEŽAL, Z., KIESLING, C., LACASTA, C., MOSER H.-G. et al.: *The Belle II PXD Whitebook*, DEPFET Collaboration, 2012

[A10] DOLEŽAL, Z., UNO, S., et al.: *Belle II Technical Design Report*, KEK Report 2010-1, 2010

[A11] The ILD Concept Group: *The International Large Detector – Letter of Intent*, KEK Report 2009-6, 2009

* Corresponding author

In Preparation

[A11] ANDRICEK, L., DOLEŽAL, Z., KOFFMANE, C., KODYŠ, P., MOSER, H-G., MÜLLER, F., NINKOVIC, J., OSWALD, C., RICHTER, R., RITTER, A., RUMMEL, S., **SCHEIRICH, J.***, WASSATSCH, A.: *Laser Tests of the DEPFET Gated Operation,* Journal of Instrumentation, 2013 (expected)

[A12] **RICHTER, R.***, ANDRICEK, L., BÄHR, A., GÄRTNER, K., KIESLING, C., KOFFMANE, C., KRÜGER, H., KREIDL, C., MOSER, H.-G., MÜLLER, F., NINKOVIC, J., PERIC, I., RUMMEL, S., SCHEIRICH, J., SCHWENKER, B., WILK, F.: *Particle Detection with DEPFET Arrays in Gated Mode*, IEEE Nuclear Science Symposium and Medical Imaging Conference, 2013 (expected)

* Corresponding author

Response and reviews

The results of the thesis were regularly presented with positive response at the DEPFET and Belle II meetings:

- 2nd International Workshop on DEPFET Detectors and Applications (2008)
- 3rd International Workshop on DEPFET Detectors and Applications (2009)
- Belle II PXD/DEPFET Meeting (2010)
- 4th International Workshop on DEPFET Detectors and Applications (2010)
- 6th International Workshop on DEPFET Detectors and Applications (2011)
- 7th International Workshop on DEPFET Detectors and Applications (2011)
- 8th International Workshop on DEPFET Detectors and Applications (2011)
- A Common Belle II SVD-PXD Meeting (2012)
- 11th Belle II General Meeting (2012)

and at the conferences:

- Topical Workshop on Electronics for Particle Physics (2009, 2011, 2012)
- 8th International Conference on Advanced Semiconductor Devices & Microsystems (2010)
- 14th International Student Conference on Electrical Engineering POSTER (2010)

Program Committee of POSTER 2010 and the MTT/AP/ED/EMC Joint Chapter of the Czechoslovakia Section IEEE awarded authors work "DEPFET Mini-matrix Particle Detector" at 14th International Student Conference on Electrical Engineering POSTER 2010.

Review of the article *Advanced Testing of the DEPFET Minimatrix Particle Detector (2011)*:

"The paper presents a new test system developed for the characterization of DEPFET sensors for the Belle II Experiment. Given the growing interest for the development of vertex detectors based on the DEPFET technology, the test system presented in this paper is certainly of general interest. The paper is well structured and reads very well. Therefore, I recommend it for publication. ..."

RÉSUMÉ

Jan Scheirich was born in 1983 in Poprad, Slovakia. He spent his bachelor, master and doctoral studies at the Czech Technical University in Prague. His doctoral studies were carried out in cooperation with Charles University in Prague where he participated on development of DEPFET particle detector for Belle II experiment in Tsukuba, Japan. He was selected to CERN Summer School Programme in 2007 where he developed fast high voltage switches for RFQCB (Radio Frequency Quadrupole ion Cooler and Buncher) at ISOLDE experiment. He participated in two successful students stratospheric balloon campaigns BEXUS-7 and -9 (Balloon EXperiments for University Students) carrying MEDIPIX and TIMEPIX particle detectors, sponsored by German Aerospace Center, Swedish National Space Board and European Space Agency in 2008 and 2009. The launch campaigns took place in Swedish Space Center ESRANGE. He was offered a research fellowship by the European Space Agency in 2010, where he did research on a Power Distribution Unit for the Large Space Simulator situated in the European Space Agency's European Space Research and Technology Center in the Netherlands. His PhD research was partially financed by three grants (2010 - 2012) which he had won in the Student Grant Competition of the Czech Technical University in Prague (GS10/075/OHK3/1T/13, SGS11/066/OHK3/1T/13, GS12/073/OHK3/1T/13). He participated on a research grant of Czech Science Foundation (203/10/0777 2010 – 2012) and on a grant of Foundation of Ministry of Education, Youth and Sports of the Czech Republic (LA10033 2010 – 2012). He was awarded by Program Committee of POSTER 2010 and the MTT/AP/ED/EMC Joint Chapter of the Czechoslovakia Section IEEE at 14th International Student Conference on Electrical Engineering POSTER 2010 for the work "DEPFET Mini-matrix Particle Detector". He is member of DEPFET Collaboration and he has been collaborating with Max-Planck Institute in Munich, Bonn University, Ludvig-Maximilians University in Munich, KEK Laboratory in Japan, CERN in Switzerland and others during his PhD studies.

Anotace

Probíhající inovace japonského částicového experimentu Belle v KEK B-Factory, Belle II, bude využívat srážek asymetrických svazků elektronů a pozitronů k produkci párů B a anti-B mezonů. Potvrzení existence nových částic studiem fyziky těžkých kvarků měřeními s velkým množstvím událostí se plánuje v experimentu Belle II. V detektoru Belle II, který měří typ, dráhy, moment hybnosti a energii nově vzniklých částic, bude využit nový typ křemíkového pixelového detektoru DEPFET (DEPleted Field Effect Transistor), předpovídaného v roce 1987 Kemmerem a Lutzem. DEPFET senzor, který obsahuje MOSFET (Metal Oxide Semiconductor Field Effect Transistor) integrovaný v každém pixelu, představuje nový koncept aktivního pixelu s nízkým šumem za pokojové teploty, nedestruktivního opakovaného vyčítání a ztenčované technologie.

Na testování a charakterizaci prototypů DEPFET senzorů byl navržen test systém nazvaný Mini-matrix system. Tento systém má celkový šum 20 elektronů ekvivalentního vstupního nábojového šumu. Systém dokáže ovládat 48 aktivních pixelů senzoru pomocí konfigurovatelných sekvencí s vysokým časovým rozlišením. V systému je integrována počítačem řízená polohovatelná optická hlavice umožňující skenování povrchu detektoru laserovým svazkem a počítačem řízené napájecí zdroje, pro automatická měření. Dvě generace detektorů PXD5 a PXD6 byly testovány na Mini-matrix systému v letech 2010-2012 a výsledky byly použity k charakterizaci senzorů a pro nové návrhy detektorů.

Na Mini-matrix systému byly proměřeny elektrické charakteristiky DEPFET senzoru, byly provedeny studie závislosti ztráty náboje na hranách detektoru na bulk napětí a odezvy na sběr náboje v rámci jednotlivých pixelů. Linearita DEPFET senzoru byla potvrzena pulzním laserem s modulací šířky pulzů a senzor byl kalibrován radioaktivními zdroji záření. Provoz DEPFET senzoru v „hradlovém režimu“ (gated operation) byl poprvé testován na Mini-matrix systému. Ve standardním provozu DEPFET senzor integruje náboj kontinuálně. Hradlový režim provozu DEPFET senzoru umožňuje znecitlivění senzoru na příchozí radiaci na přesně definovaný časový interval. Náboj uložený v interním hradle senzoru zůstane zachován a integrace náboje může pokračovat po ukončení necitlivé fáze. Tento rychlý mechanizmus, kterým lze definovat časové okno, v němž detektor neintegruje nově generovaný náboj, může být například využit k odstínění nově injektovaných shluků částic v urychlovači, které způsobují rušení detektoru. Hradlový režim provozu zásadním způsobem rozšiřuje využití DEPFET senzoru a nemá obdobu u jiných světových pixleových senzorů.

Měření DEPFET senzorů provedená na Mini-matrix systému vedla k jedinečným výsledkům a hlubšímu porozumění DEPFET senzoru. Vývoj nové rozšířené verze Mini-matrix systému byl zahájen a očekává se, že přinese ještě detailnější měření DEPFET senzorů. Vývoj aktivního pixelového detektoru vedeného DEPFET Collaboration se blíží ke konci a očekávaný start experimentu je v roce 2015.